MEASUREMENTS OF THE ^{3}He FUSION PRODUCT IN TFTR

J. D. Strachan

Plasma Physics Laboratory, Princeton University

Princeton, New Jersey 08543

PPPL--2544

DE89 004617

ABSTRACT

The 0.8-MeV ^{3}He ion created in the d(d,n)^{3}He fusion reaction is confined in TFTR and can undergo d(^{3}He,p)α fusion reactions. The time evolution, and profile of the 14.7-MeV proton emission indicates that collisional energy transfer with plasma electrons is the dominant process influencing the charged ^{3}He fusion product for TFTR plasmas and that there is no observable anomalous transport. The magnitude of the burnup exceeds classical expectations by a factor-of-two-to-three which is a little beyond experimental uncertainties.

INTRODUCTION

One goal of fusion plasma experiments is to understand the conditions necessary for ignition. One condition for ignition of a deuterium-tritium (d-t) plasma is that the 3.5-MeV alphas be confined for times longer than that required to transfer most of its energy to the bulk plasma. A related topic is the confinement of deuterium fusion products [1]. These ions have orbits, collision rates, and birth profiles that are similar to the d-t alphas; however, the density of the d-d charged particles is much lower so that effects due to alpha pressure and alpha-induced interactions do not occur. The confinement of the 1-MeV triton from the d(d,p)t fusion reaction has been studied in PLT [2,3], PT [4], TFTR [5], and JET [6]. The confinement of the 0.8-MeV ^{3}He ion from the d(d,n)^{3}He fusion reaction has been studied previously only in PDX. In that device the behavior was consistent with classical confinement [3] except in the presence of fishbone MHD events [7] where some anomalous losses were inferred. In this paper, measurements of the 0.8-MeV ^{3}He fusion products in TFTR are reported.

The confinement properties of the 0.8-MeV ^{3}He ion are inferred from the simultaneous measurement of the 2.45-MeV neutron emission (which monitors the ^{3}He ion creation rate) and the 14.7-MeV proton emission (which monitors the subsequent ^{3}He ion burnup as it slows down through the peak of the d-^{3}He cross section at 0.6 MeV). If the ^{3}He ion is confined inside the TFTR plasma, then it has about 0.1 - 0.3% probability of undergoing the subsequent d(^{3}He,p)α fusion reaction. If the ^{3}He ion is unconfined, then it has about 10^{-6}% probability of undergoing the d-^{3}He fusion reaction with deuterium sorbed in the vessel wall or the limiter [2]. Thus, the observation of the magnitude of the 14.7-MeV proton emission (^{3}He burnup) indicates the number of ^{3}He ions that exist in the plasma with energies near the peak of the d^{3}He reactivity.

These TFTR results are consistent with classical behavior dominated by electron drag such that the energetic ^{3}He ions lose energy collisionally before they experience observable cross-field transport. However, TFTR measurements do not exist for types of plasmas that have been associated with anomalous losses of energetic ions [3,7]. The present TFTR data are an improvement over the earlier PDX ^{3}He measurements [3,7] since better time resolution and some spatial resolution have been obtained. Also, documentation from a number of TFTR plasmas has allowed measurements of the dependence on electron temperature.

EXPERIMENT

The results in this paper were obtained from TFTR, operated (except where otherwise noted) with a major radius of 255 cm, plasma minor radius of 83 cm, and top-bottom carbon rail limiters [8]. The TFTR parameters included toroidal magnetic fields up to 5 Tesla, plasma currents up to 2.2 MA, and up to 5 MW of co-tangential deuterium neutral beam heating [9].

The 2.45-MeV neutron emission (0.8-MeV ^{3}He ion creation rate) was measured by large NE102A- and ^{6}Li-loaded ZnS scintillators [10] normalized to the calibrated TFTR epithermal neutron detectors [11,12]. The total uncertainty in the neutron measurement is in the range of 10% [12]. The escaping 14.7-MeV protons (^{3}He ion burnup rate) were detected by an array of surface barrier detectors at the bottom of the TFTR vacuum vessel [13]. For the TFTR magnetic field orientation, the energetic ions grad-B-drifted to the bottom of TFTR. The array consisted of four detectors displaced in major radius in order to obtain spatial profile information. One of the detectors was unable to accept the energetic protons [13] and was used to evaluate the neutron noise in the detectors. The available spatial resolution was

approximately the 14.7-MeV proton gyrodiameter (≈ 30 cm). The data were collected in 2.5-msec time bins; however, the actual time resolution was often limited by counting statistics and often several time bins were added together to gain better statistics at the expense of time resolution. Typical time resolution was as good as 5-msec.

Absolute calibration of the magnitude of the 14.7-MeV proton signal was obtained by puffing known amounts of ^{3}He gas into TFTR using the method developed on PDX [3]. Those gas puffs were also used to analyze ^{3}He particle transport [14]. The basic idea was to puff a known, trace amount of ^{3}He into a deuterium plasma that is heated by deuterium neutral beams ($D^o \rightarrow D^+$) where the neutron emission is dominated by beam-target reactions. In that case, the total d-^{3}He reaction rate was calculated from the ratio of the d-^{3}He and d-d cross sections, the measured d-d neutron rate, and the ^{3}He and deuterium densities without further numerical modelling. The d-^{3}He reactivity during the calibration is between the energetic beam ions and the rotating thermal ^{3}He ions while the burnup reactions occur with energetic ^{3}He ions near the peak of the d-^{3}He cross section (≈ 400-keV) and rotation of the thermal deuterons has a smaller influence. These differences in the reaction energies is unimportant except that the 14.7-MeV protons will have a slightly broader energy distribution for the case of the burnup reactions which can slightly change the spatial origin (orbits) of the detected protons. The magnitude of the total yield was determined only by the detector which was most sensitive to the central plasma region. The actual profile of the reactions is relatively unimportant since we are assuming that by accessing the central plasma regions, the detector signal approximates the sum over the plasma volume. In principle, the d-^{3}He rate could be calibrated to about 75% accuracy with the uncertainty in the deuteron density being the largest source

of error. In fact, the ^{3}He density was probably an even bigger uncertainty, and we ascribe a factor-of-three uncertainty in the calibration to our knowledge of this term. Our accuracy of determining the amount of ^{3}He puffed into the vessel in test conditions was about 20% and was reproducible. However, the density rise associated with that same gas valve settings during machine operation was caused by only one-third as many particles as were thought to be puffed. Further, the results of the ^{3}He particle transport experiment [12] suggested that ^{3}He was 100% recycled and was not being stored in the limiters and walls. Since these observations are discrepant, we have taken the number of ^{3}He particles to be one-half of the electron density rise associated with the ^{3}He puff and take the difference between that value and the value associated with the valve calibration as the uncertainty. Essentially, this amounts to assessing the discrepant observations to the valve performance being different during plasma operation when stray magnetic fields of up to 5-kG occur. The outside detectors were calibrated relative to the central detector. The relative calibration yielded the emission profile for a thermal ^{3}He density profile (presumably near parabolic for these plasmas) with the neutral beam deposition profile and, thus, allowed us to measure the burnup profile in relation to the calibration profile.

The data reported in this paper represent all the presently available ^{3}He burnup data on TFTR. One case from this data set was included in Ref. [1]. The data were obtained in the spring of 1985. Subsequent use of the surface barrier detectors has been difficult due to prompt gamma noise from the larger neutron emissions on TFTR and the cumulative radiation damage in the detectors. Future TFTR measurements of the escaping 14.7-MeV protons will use the radiation resistant detectors [15] developed for detection of escaping alphas.

RESULTS

The time evolution of the burnup signals are plotted in Fig. 1 for a 5.2-T, 0.8-MA TFTR plasma heated with 5.3-MW of co-deuterium neutral beams. The 0.8-MeV ^{3}He ion creation rate (2.5-MeV neutron emission rate) had a steady-state value of $2.7 \pm 0.3 \times 10^{14}$ sec^{-1}. The count rate in the proton detectors is sizeable ($\sim 10^4$ cps), and is about ten times larger than occurred on PDX, making it possible to follow the d^{3}He emission level over about three orders of magnitude. The plasma conditions and ^{3}He creation rate approached steady state for the final 0.3 sec of the beam heating with, however, the line-averaged density rising modestly (Fig. 1). The 0.3-sec duration was sufficient for the ^{3}He ion population to reach equilibrium. In fact, in Fig. 1, the 14.7-MeV proton signals were in equilibrium for the final 0.1 sec of the beam heating.

The magnitude of the d-^{3}He fusion reaction rate in Fig. 1 is in the range of $1 \rightarrow 4 \times 10^{11}$ 14.7-MeV p/sec for a burnup rate of $0.4 \rightarrow 1.6 \times 10^{-3}$. These values are comparable to the 0.8-MeV ^{3}He burnup expected ideally for a 3-keV plasma which is in the range of $0.7 \rightarrow 1 \times 10^{-3}$ [1]. In this case, "ideal" means that there are no impurities in the plasma, and that all the ^{3}He is located in the plasma center. The ideal value is expressed as a range due to the uncertainty in the measurement of the central electron temperature. The actual theoretical burnup values are often about one-half of the ideal value due to profile effects and, principally, the depletion of the background deuterium by impurities. The dashed line in Fig. 1 is a code calculation [3] of the time evolution of the predicted d^{3}He reaction rate which indicated equilibrium burnup values of $0.15 \rightarrow 0.4 \times 10^{-3}$, where the range in the calculated burnup results from the uncertainty in the deuteron density.

The magnitude of the steady-state burnup (Fig. 2) is about equal to the ideal value and exceeds the classical calculation by a factor of up to three. This excess is only slightly more than the uncertainty in the absolute calibration of the proton detectors. In light of the burnup measurements exceeding the expected burnup calculations, it is natural to ascribe the difference to the absolute calibration. In fact, the absolute calibration has a high degree of uncertainty and, moreover, is necessarily pertubative since it requires a measurable density rise (~5% in these plasmas). However, it cannot be overlooked that there are difficiencies in the burnup calculation principally with the exclusion of energetic-deuterium with energetic ^{3}He reactions and exclusion of rotation effects. The data in Fig. 2 exhibited a dependence on electron temperature that is consistent with ideal dependence ($T_e^{3/2}$) due to electron drag. There were no other observable dependence within the data, which included a beam power scan up to 5-MW, and a range of toroidal magnetic fields between 4.0 and 5.0-T. All of the data in Fig. 2 are restricted in plasma current to be above 0.65-MA and below 1.35-MA. Normalizing the raw counting rate to the source rate, Fig. 3 indicates that lower burnup values were obtained at higher and lower currents. Our interpretation is that at the lower plasma currents, the classical orbit losses of the 0.8-MeV ^{3}He ions becomes important in reducing the burnup, as was observed on PDX [3]. At the higher plasma currents, the escaping 14.7-MeV protons originate from the plasma periphery since the central protons are confined. In Fig. 3, the minimal minor radius of the detected 14.7-MeV protons is also indicated. Thus, by restricting the plasma current to less than 1.35 MA, we restrict the origin of the detected protons to be within $r/a \leq 0.25$. The detected orbits are all of trapped 14.7-MeV protons which leave the plasma before encountering their banana tips. The actual confinement of

the entire 14.7-MeV proton population is less than 50% and is not changed much by increasing the plasma current to 1.8-MA. However, the orbits available to the detectors do move out in major radius since at the higher plasma currents, protons from the same locations encounter their banana tips and leave the plasma at different locations (see Ref. 13 for typical detected orbits).

The major radial displacement of the proton detectors on TFTR, along with the fact that the 14.7-MeV proton gyroradius was smaller than the plasma minor radius, allowed spatial resolution of the order of the proton gyrodiameter to be obtained [13]. As can be seen by the orbits (Fig. 3 in Ref. [13]), the 14.7-MeV protons detected by the detector right under the minor axis (central detector) pass through the center of the plasma while the orbits of the 14.7-MeV protons detected by the detector at +40 cm (off-axis detector) only pass to as close as 25 cm from the plasma center. The raw count rate for the off-axis detector (Fig. 1) is about an order of magnitude smaller than the central detector count rate. This indicates that the d-^{3}He emission is strongly peaked on axis much as expected since the ^{3}He source is centrally peaked (Figs. 1 and 4). Calculation (using the code of Ref. [3]) of the off-axis count rate indicates higher than experimental values for times early in the neutral beam injection possibly since the d-d source profile in the calculation has been constant in time at the value associated with the measured Thomson scattering profiles (at 3.2 sec). Those profiles are probably broader than occurred at the beginning of the beam heating when the density was lower and the neutral beam deposition more peaked. The data for the off-axis detector was not recorded between 3.2 and 3.35 sec when a baseline shift made the electronic counting system inoperative. The calculated burnup profile (Fig. 4) is narrower than the source profile by the factor of $[T_e(r)/T_e(0)]^{3/2}$ to account for the ^{3}He slowing down faster in the

outer plasma regions. The data in Figs. 1 and 4 are consistent with the ^3He having undergone little transport during its burnup.

The ratio of off-axis to central counts is plotted in Fig. 5 as a function of plasma current. The ratio, (R), of off-axis to central counts during the ^3He puffing calibration can be related to the theoretically expected burnup ratio:

$$R^{theory} = R^{calibration} \left(\frac{T_e(r)}{T_e(o)}\right)^{3/2} ,$$

where the principal further assumption is that during the ^3He puffing calibration the ^3He density had the same profile shape as the electron density. This ratio is independent of the beam deposition profile and the deuteron depletion uncertainties and, thus, is a relatively accurate assessment of the spatial distribution of the energetic ^3He ions. The principal result is that the ratio of off-axis to central counts is close to the calculated value for all cases where a ^3He puffing calibration was performed (Fig. 5) as if no transport of the ^3He ions occurred. A bound on the magnitude of any ^3He transport can be inferred from the data in Fig. 5. In order for little transport to occur from the central detector to the off-axis detector (about 25 cm, Fig.6) in a time scale of the cross-section-weighted slowing-down time, the ^3He ion diffusivity must be less than 10^4 cm^2/sec.

The time scale for the ^3He ions to lose their energy can be inferred from the time delay of the burnup signal with respect to the ^3He creation rate (Fig. 1). This delay is evident in the beginning and the termination of the neutral beam heating. The delay time (Fig. 7) at the termination of the beam heating lasts as the ^3He source is reduced by several orders of magnitude and

is approximately 75 ms-.c for the plasma in Fig. 1. The evolution of the plasma during the decay (Fig. 7) has uncertainty due to the time evolution of Z_{eff}, and the density profile. Consequently, the modelling of the decay of the ^3He burnup has some uncertainty. A range of possible burnup evolutions from the code of Ref. [3] are shown in Fig. 8, and the calculations tend to decay a little faster than the experimental data.

Approximately, the delay time (Fig.7) is the time for the ^3He ions to cool until they have a low probability of undergoing a $d(^3He,p)\alpha$ fusion reaction. The measured delay time is about 60% of the time for the central ^3He ions to cool from 0.8-MeV to 0.4-MeV (Fig. 9). Since electon drag is the dominant collisional process, this time scales as $T_e^{3/2}/n_e$, and the experimental data exhibit this variation over about an order of magnitude. Furthermore, the energetic injected ions from the neutral beams are governed by the same process, and the experimental burnup delay time about equals the exponential neutron decay time observed at the beam turn-off (Fig. 9). Collisionally, it should take the ^3He ions 10% longer to cool to 0.4-MeV than for the 0.1-MeV deuterons to cool to 0.07-MeV (which is about 1/e in the d-d fusion reactivity).

The time evolution of the ^3He burnup was recorded during a plasma which was fueled by a deuterium pellet [16]. During $D^0 \rightarrow D^+$ neutral beam heating, the pellet transiently increased the beam-target 2.45-MeV neutron emission and, subsequently, fell due to the reduced beam penetration and the lower electron temperature [16]. The 14.7-MeV proton emission had the same increase and subsequent decay for the same physical reason. The ^3He burnup is temporarily increased (Fig. 10) due to the increased deuterium target for the existing energetic ^3He ions, and the magnitude of the increase was similar to the magnitude of 2.5-MeV neutron increase. The 14.7-MeV proton emission is

subsequently reduced due to the reduced creation rate. Essentially, the data in Fig. 10 indicate that the pellet did not have a significant adverse effect on the confinement of the ^{3}He fusion product.

The time evolution of the ^{3}He burnup (Fig. 11) was also recorded for a TFTR compression case of the free-expansion type [17]. For this case, the outside proton detector [13] observed the center of the precompressed plasma, and the motion of the plasma towards the center of the vacuum vessel caused this detector to subsequently view protons emitted from about half of the minor radius. Conversely, the detector located under the center of the plasma viewed the outer region of the precompressed plasma and the central region of the post-compressed plasma. The net result is that the compression caused the outer signal to reduce and the central signal to increase with a time constant associated with the compression. A quantitative comparison with a burnup code [3] is difficult since the plasma motion changes the detector calibrations. However, one can probably conclude that a drastic loss of ^{3}He ions did not occur at the compression since otherwise a delay of about the slowing-down time (≈ 50 msec) would be observed in the rise of the central signal. Interestingly, the 2.45-MeV neutron emission can be increased at the compression [18] due to the compressional acceleration of the beam ions. A similar increase is not observed on the 14.7-MeV protons since all the d^{3}He reactions already occur at the peak energy of the d^{3}He cross section. During the neutral beam heating phase of most of these plasmas, there were no sawtooth MHD activity. However, following the neutral beam heating (e.g., the first post-heating sawtooth occurred at 3.3-sec in Fig. 7) the sawtooth activity would begin again. No correlation of the burnup signal (Fig. 7) was observed with the sawtooth activity unlike the observations on JET [19].

CONCLUSIONS

The TFTR ^3He burnup data extend existing charged fusion product data to include better counting statistics, time resolution, and profile information. All data can fit calculations based upon collisional energy transfer to the plasma electrons being the dominant process influencing the energetic ^3He ions. The principal deviations (which are near the experimental uncertainties) is that the magnitude of the burnup exceeds expected values by a factor-of-two-or-three. This difference may also reflect the inadequacies of our present burnup modelling to deal with rotation and enhanced burnup reactions between the ^3He ions and the energetic beam ions.

The measured burnup profiles are consistent with those expected without any ^3He transport indicating that if diffusive transport of the ^3He ion occurs then the diffusion coefficient is less than 10^4 cm^2/sec. The time evolution of the burnup at beam turn on and off are consistent with electron drag being the dominant transient time scale in the evolution of the ^3He burnup.

ACKNOWLEDGMENTS

The author appreciates technical support from R. Waszazak and J. Roberts. The support of K. Young, D. Johnson, and G. Taylor, who supplied plasma diagnostic information, is gratefully acknowledged. The author also appreciates useful discussions with W. Heidbrink and H.-S. Bosch, who ran the burnup code.

This work was supported by the U.S. Department of Energy Contract No. DE-AC02-76-CHO-3073.

REFERENCES

[1] STRACHAN, J.D., CHAN, A.A., HEIDBRINK, W.W., LOVBERG, J., MURPHY, T.J., NIESCHMIDT, E.B., and ZWEBEN, S.J., Basic Physical Processes of Toroidal Fusion Plasma (Varenna, 1985) EUR-10418 EN.

[2] COLESTOCK, P.L., STRACHAN, J.D., ULRICKSON, M., and CHRIEN, R.E., Phys. Rev. Lett. 43 (1979) 768.

[3] HEIDBRINK, W.W., CHRIEN, R.E., and STRACHAN, J.D., Nucl. Fusion 23 (1983) 917.

[4] BITTONI, E., FUBINI, A., HAEGI, M., PEDRETTI, E., PILLON, M., and VANNUCCI, A., in Proceedings of the 12th European Conference on Controlled Fusion and Plasma Physics, Budapest, 1985, Vol. I, p. 211.

[5] JASSBY, D.L. et al., in Proceedings of the 14th European Conference on Controlled Fusion and Plasma Physics, Madrid, 1987.

[6] BATISTONI, P. et al., in Proceedings of the 14th European Conference on Controlled Fusion and Plasma Physics, Madrid, 1987, Vol. III, p. 1228.

[7] HEIDBRINK, W.W., HAY, K., and STRACHAN, J.D., Phys. Rev. Lett. 53 (1984) 1905.

[8] YOUNG, K.M. et al., Plasma Phys. Controlled Fusion 26 (1984) 11.

[9] MURADAMI, M. et al., Plasma Phys. Controlled Fusion 28 (1986) 17.

[10] HEIDBRINK, W.W., Rev. Sci. Instrum. 57 (1986) 1769.

[11] HENDEL, H.W., IEEE Trans. Nucl. Sci. 33 (1986) 670.

[12] NIESCHMIDT, E.B., KU, L.P., and TSANG, F.Y., Rev. Sci. Instrum. 56 (1985) 1084. Subsequent calibration work has indicated that the uncertainty in the $d(d,n)^3He$ 2.5-MeV neutron calibration may be larger than 10% and as large as 30-50%.

[13] STRACHAN, J.D., Rev. Sci. Instrum. 57 (1986) 1771.

[14] STRACHAN, J.D., and CHAN, A., Nucl. Fusion 27 (1987) 1025.

[15] ZWEBEN, S.J., Rev. Sci. Instrum. 57 (1986) 1774.

[16] HEIDBRINK, W.W., MILORA, S.L., SCHMIDT, G.L., SCHNEIDER, W., and RAMSEY, A., Nucl. Fusion 27 (1987) 3.

[17] TAIT, G. et al., Plasma Physics and Controlled Nuclear Fusion Research (IAEA, Vienna, 1984), Vol. I, p. 141.

[18] WONG, K.L. et al., Phys. Rev. Lett. 55 (1985) 2587.

[19] KALLNE, J. et al., Physica Scripta T16 (1987) 160.

FIGURES CAPTIONS

FIG. 1. Time evolution of the 2.45-MeV neutron emission (0.8-MeV ^{3}He creation rate), the central 14.7-MeV proton emission (central ^{3}He burnup rate), and off-axis (> 25 cm) 14.7-MeV proton emission (outer ^{3}He burnup) for a low density ($\bar{n}_e$ = 1.5 x 10^{13}cm^{-3}), 4.5-MW D^0 → D^+ neutral-beam-heated TFTR plasma at 0.8 MA and 4.5 T. The outer proton detector has no signal from 3.2 to 3.3 sec due to electronic noise. The dashed line is the calculated burnup using the code in Ref. 3, and has been normalized to the central data at 3.2 sec. The calculations represent the total proton emission from the plasma and the total emission outside 25 cm while the measurements are the proton emission along a birth profile described by the 14.7 MeV proton orbits.

FIG. 2. The magnitude of the ^{3}He burnup as a function of central electron temperature. The solid line is the expected "ideal" value [5]. The shaded region is the range of predicted classical values using the theory of Ref. [3].

FIG. 3. The magnitude of the ^{3}He burnup normalized to $T_e^{3/2}$ (dependence in Fig. 2) as a function of plasma current or alternatively, the minimum radius of the plasma that the orbit of the detected 14.7-MeV proton could originate.

FIG. 4. (a) Deuterium density profile and energetic ion density profile for the plasma in Fig. 1 at 3.2 sec. The deuterium density profile is reduced from the measured electron density profile by the impurities. The energetic ion density profile is calculated from the neutral beam deposition codes.

(b) The 0.8-MeV ^{3}He source profile (approximately the product of the deuterium and energetic ion profiles), the expected burnup profile [approximately the source profile weighted to $T_e^{3/2}(r)$], and the measured profile normalized to unity at the largest values.

FIG. 5. Ratio of counts for the outer detector over the central detector as a function of plasma current and, therefore, the minimum minor radius of 14.7-MeV protons that can be detected by the outside detector (see Fig. 6). The solid line (with open points) is the ratio obtained during the calibration multiplied by $[T_e(r)/T_e(o)]^{3/2}$. The solid line then is the ratio expected if there were no energetic ^{3}He transport.

FIG. 6. Minimum accessible 14.7-MeV proton orbits for the central and off-axis detectors as a function of plasma current.

FIG. 7. Time evolution of the ^{3}He creation and burnup near the time of the neutral beam turn off (3.2 sec). The signals have been normalized at the equilibrium burnup level (3.1 → 3.2 sec). The measured delay times are indicated as that which occurred long after the beams turned off (3.4 sec).

FIG. 8. Time evolution of the calculated ^3He burnup for the data in Fig. 7. The calculation [Ref. 3] assumes classical electron drag and no ^3He transport. The solid line assumes that the density profile became parabolic and that Z_{eff} reduced to 2.0 at 3.35 sec. The long dashed line assumed that Z_{eff} rose to 4.0 at 3.35 sec. The small dashed line assumed the density profile remained unchanged and that Z_{eff} remained constant at 3.0 after the beam injection.

FIG. 9. (a) Relation of the burnup delay time (defined in Fig. 7) to the time expected for a 0.8-MeV ^3He ion to slow down sufficiently (to 0.4 MeV) for its burnup probability to have dropped to 1/e.
(b) Relation of the burnup delay time to the exponential neutron decay time.

FIG. 10. 14.7-MeV proton and 2.45-MeV neutron emission time evolution during the deuterium pellet injection into a 2-MW $D^0 + D^+$ beam-heated 0.8-MA TFTR plasma.

FIG. 11. 14.7-MeV proton emissions from a central and outside detector for the case of a small compression of the TFTR plasma from R = 290 cm to R = 255 cm.

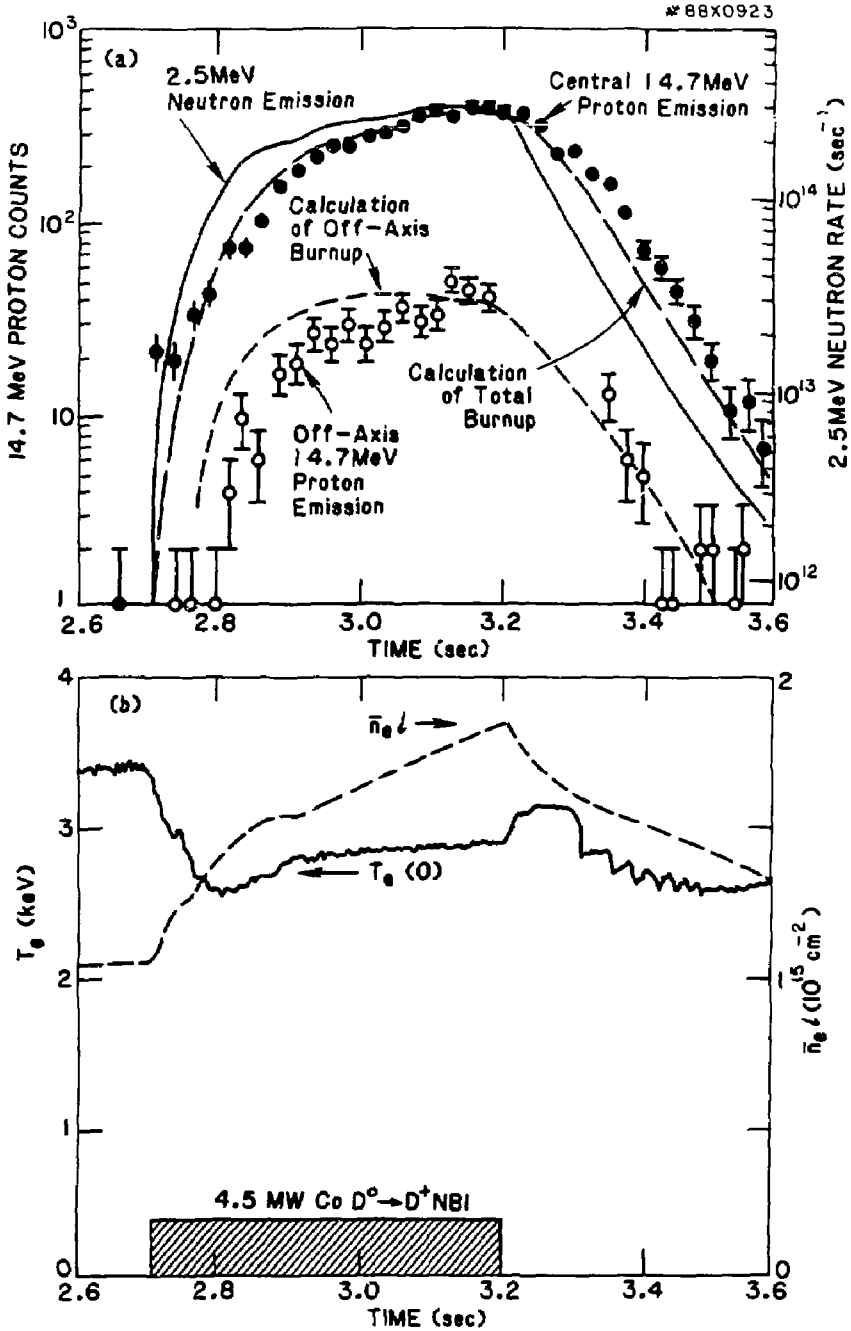
#88X0923
(a)
2.5MeV
Neutron Emission
Central 14.7MeV
Proton Emission
Calculation
of Off-Axis
Burnup
Calculation
of Total
Burnup
Off-Axis
14.7MeV
Proton
Emission
14.7 MeV PROTON COUNTS
2.5MeV NEUTRON RATE (sec⁻¹)
TIME (sec)
(b)
$\bar{n}_e l$
T_e (0)
T_e (keV)
$\bar{n}_e l$ (10^{15} cm^{-2})
4.5 MW Co D°→D⁺NBI
TIME (sec)

Fig. 1

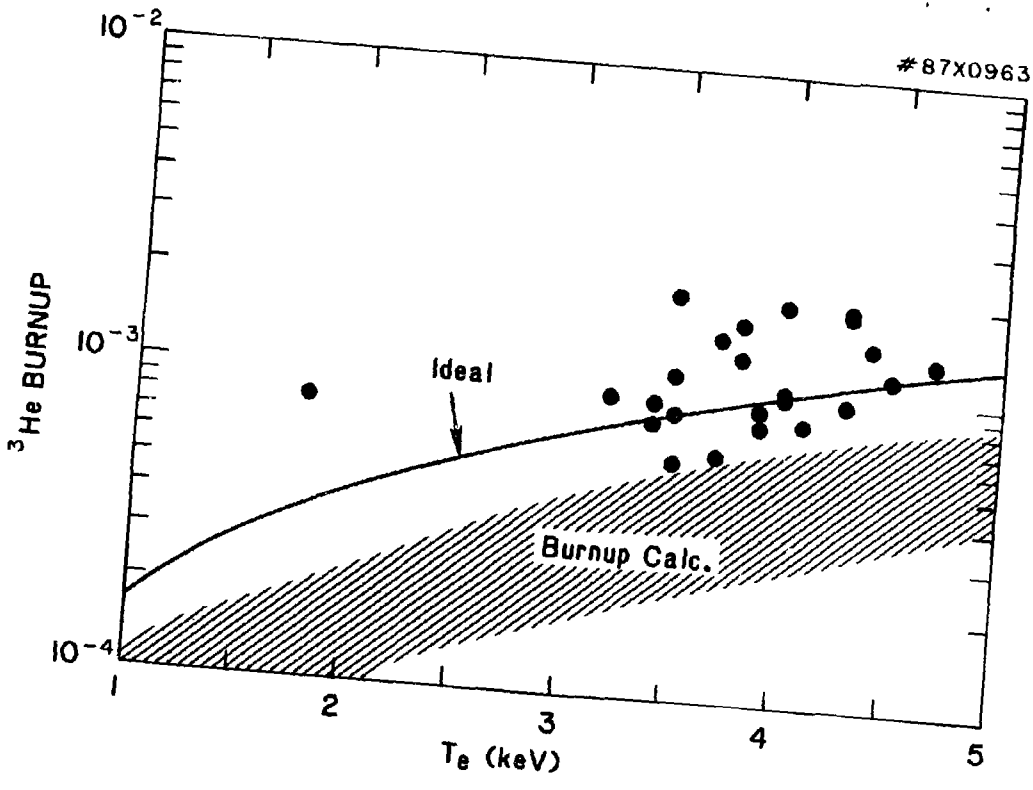
#87X0963
10^{-2}
10^{-3}
10^{-4}
^{3}He BURNUP
Ideal
Burnup Calc.
1
2
3
4
5
T_e (keV)

Fig. 2

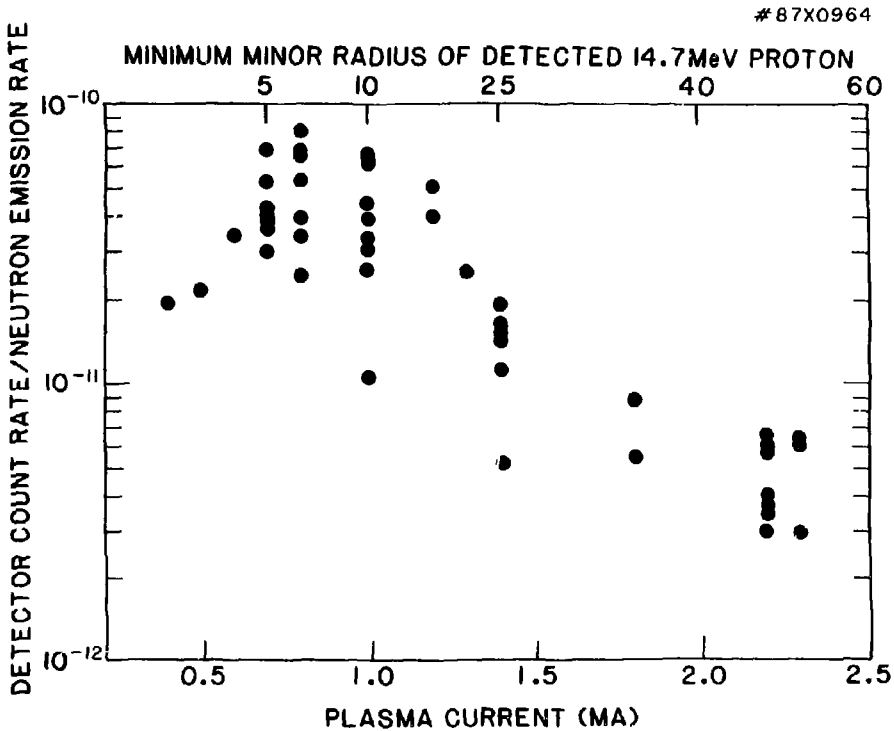
#87X0964
MINIMUM MINOR RADIUS OF DETECTED 14.7MeV PROTON
5
10
25
40
60
DETECTOR COUNT RATE/NEUTRON EMISSION RATE
10^{-10}
10^{-11}
10^{-12}
0.5
1.0
1.5
2.0
2.5
PLASMA CURRENT (MA)

Fig. 3

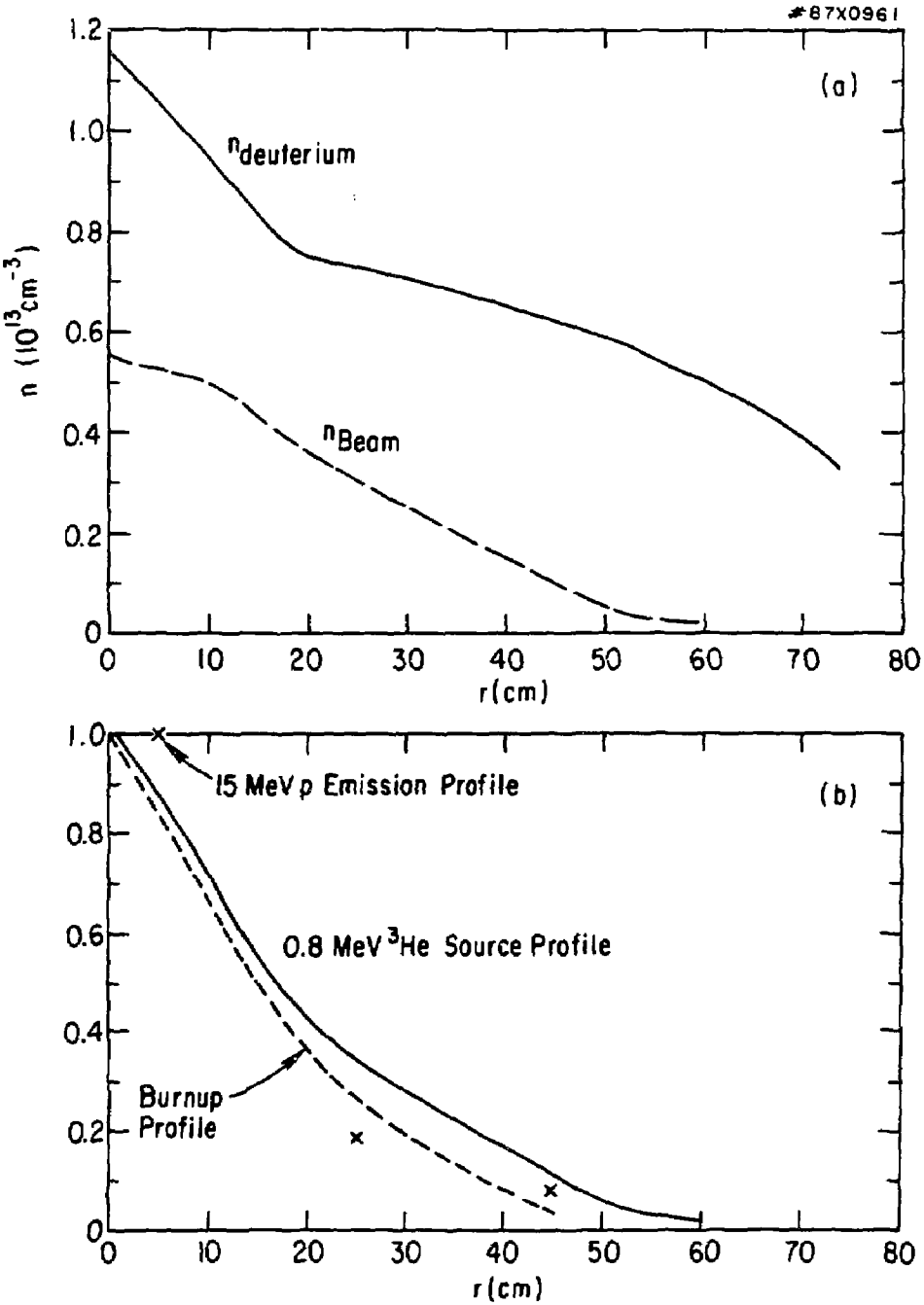
#87X0961
(a)
$n_{deuterium}$
n_{Beam}
n (10^{13}cm^{-3})
r(cm)
(b)
15 MeV p Emission Profile
0.8 MeV ^{3}He Source Profile
Burnup Profile
r(cm)

Fig. 4

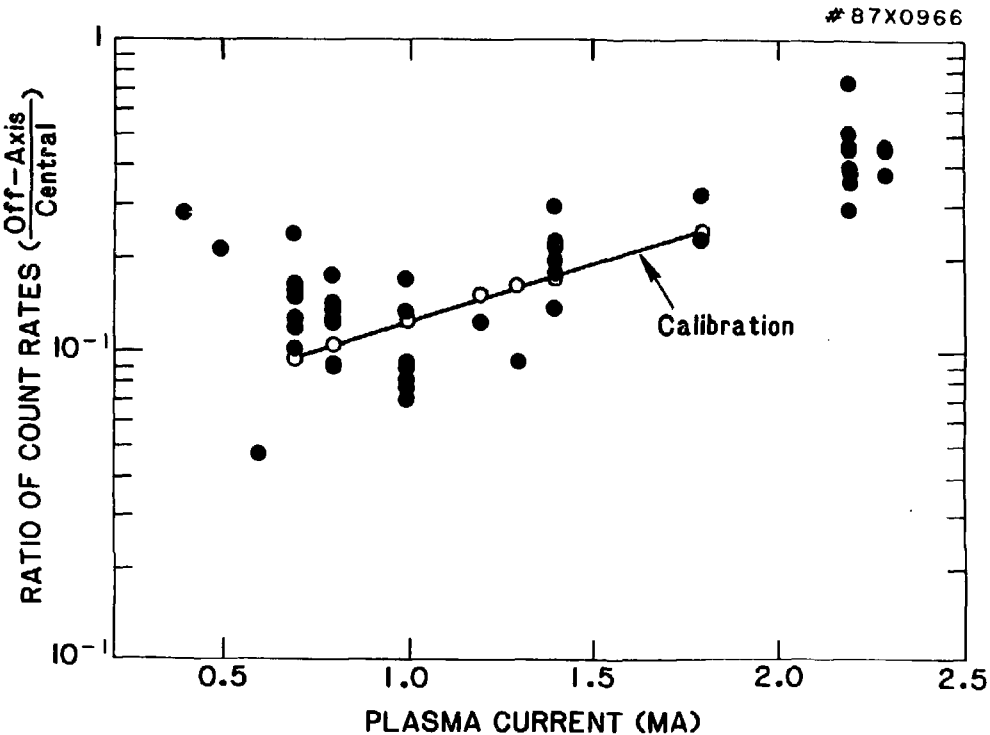
#87X0966
RATIO OF COUNT RATES (Off-Axis / Central)
1
10^{-1}
10^{-1}
0.5
1.0
1.5
2.0
2.5
PLASMA CURRENT (MA)
Calibration

Fig. 5

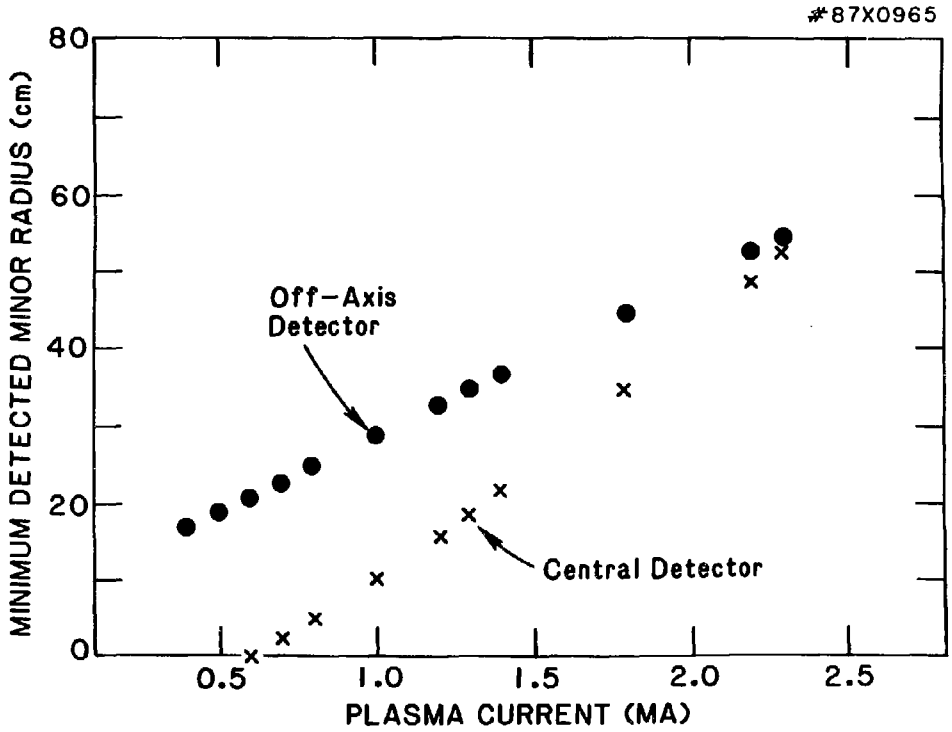
#87X0965
MINIMUM DETECTED MINOR RADIUS (cm)
80
60
40
20
0
0.5
1.0
1.5
2.0
2.5
PLASMA CURRENT (MA)
Off-Axis Detector
Central Detector

Fig. 6

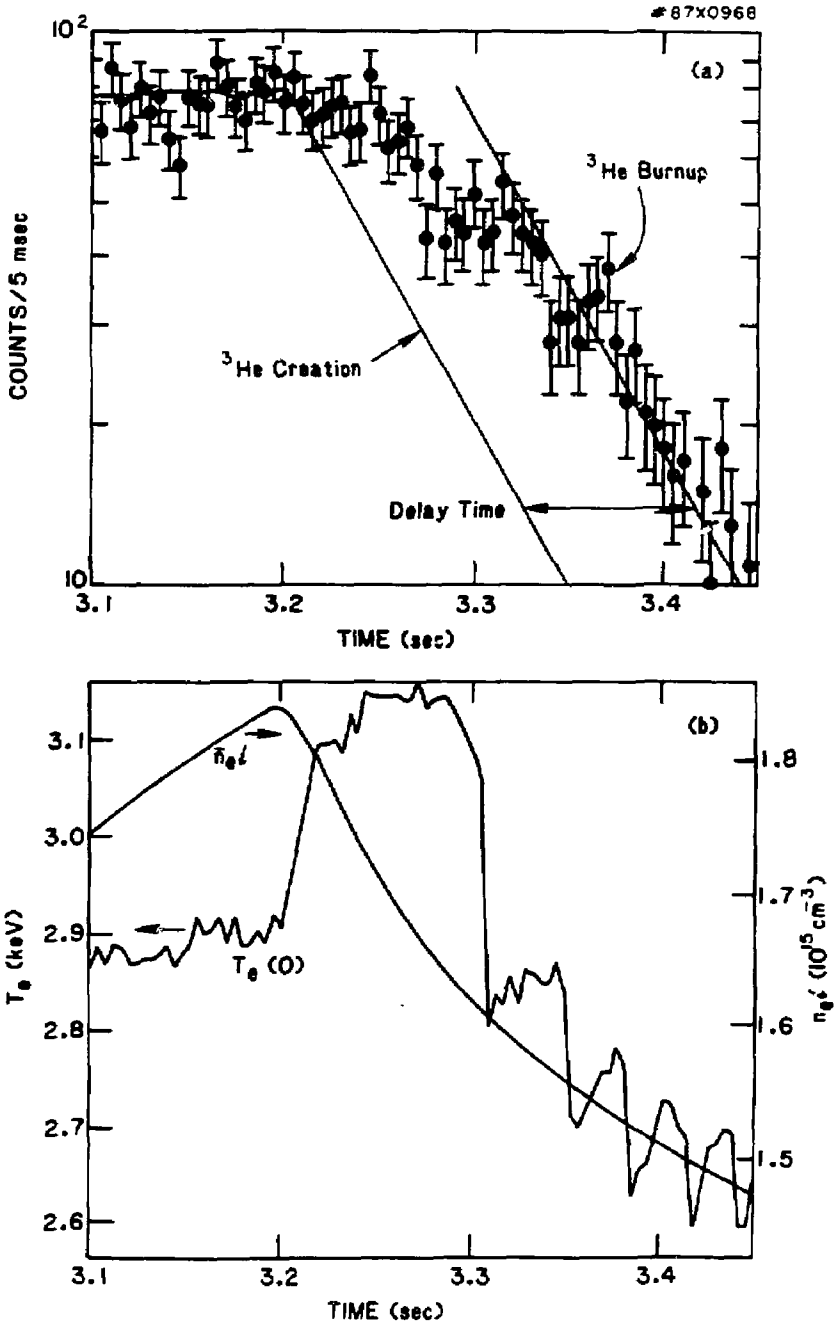
#87X0968
(a)
10^2
10
COUNTS/5 msec
^{3}He Burnup
^{3}He Creation
Delay Time
3.1
3.2
3.3
3.4
TIME (sec)
(b)
$\bar{n}_e\ell$
T_e (0)
T_e (keV)
$n_e\ell$ (10^{15} cm^{-3})
3.1
3.0
2.9
2.8
2.7
2.6
1.8
1.7
1.6
1.5
3.1
3.2
3.3
3.4
TIME (sec)

Fig. 7

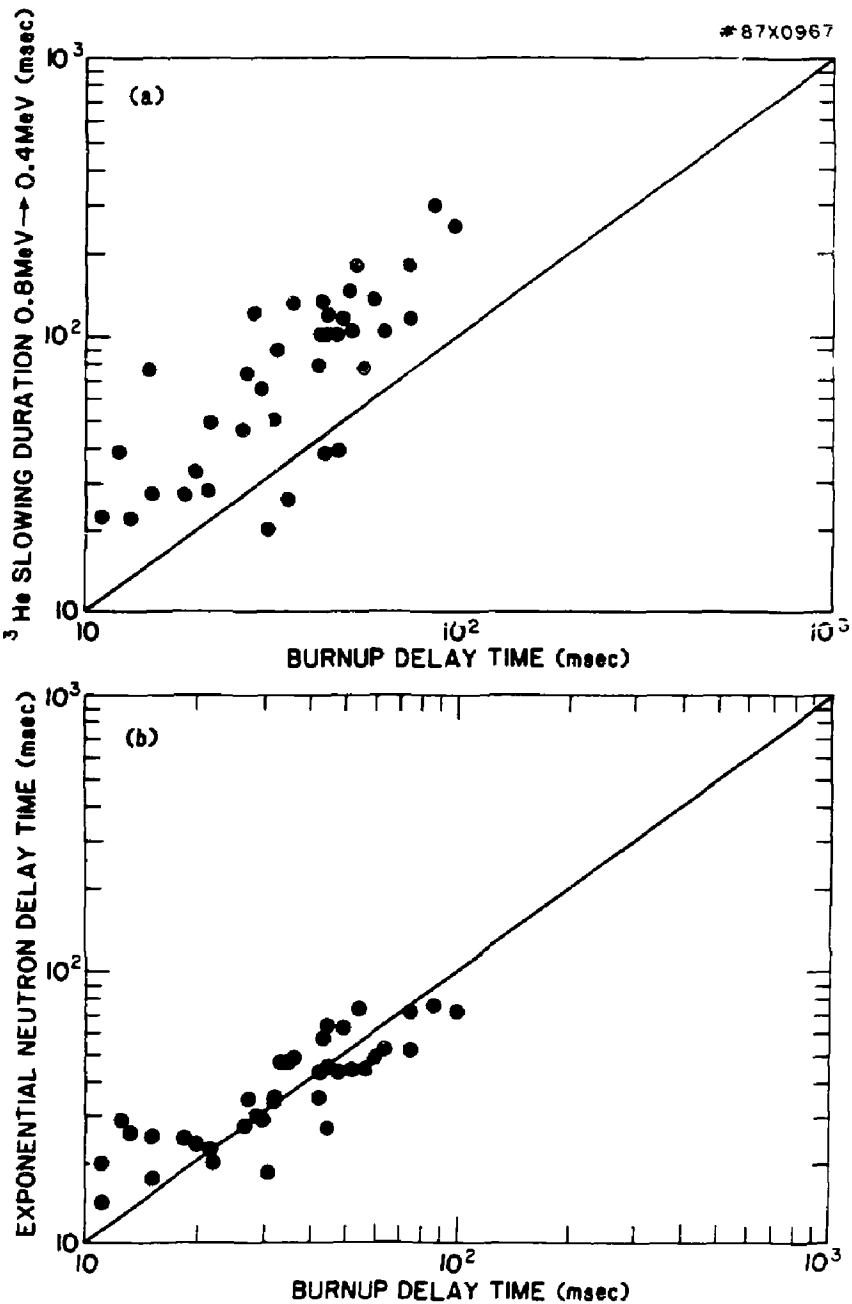
#87X0967
(a)
^{3}He SLOWING DURATION 0.8MeV→0.4MeV (msec)
BURNUP DELAY TIME (msec)
(b)
EXPONENTIAL NEUTRON DELAY TIME (msec)
BURNUP DELAY TIME (msec)

Fig. 8

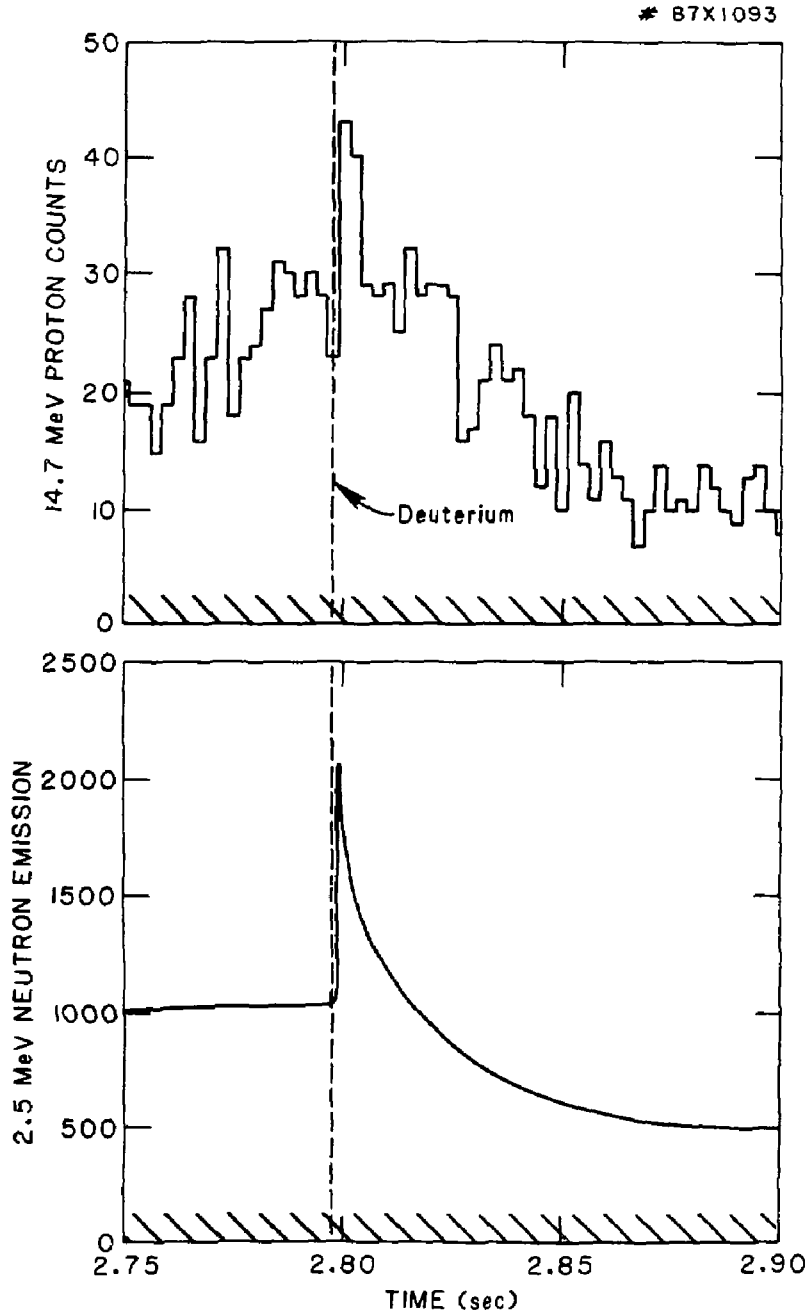
#87X1093
14.7 MeV PROTON COUNTS
50
40
30
20
10
0
Deuterium
2.5 MeV NEUTRON EMISSION
2500
2000
1500
1000
500
0
2.75
2.80
2.85
2.90
TIME (sec)

Fig. 9

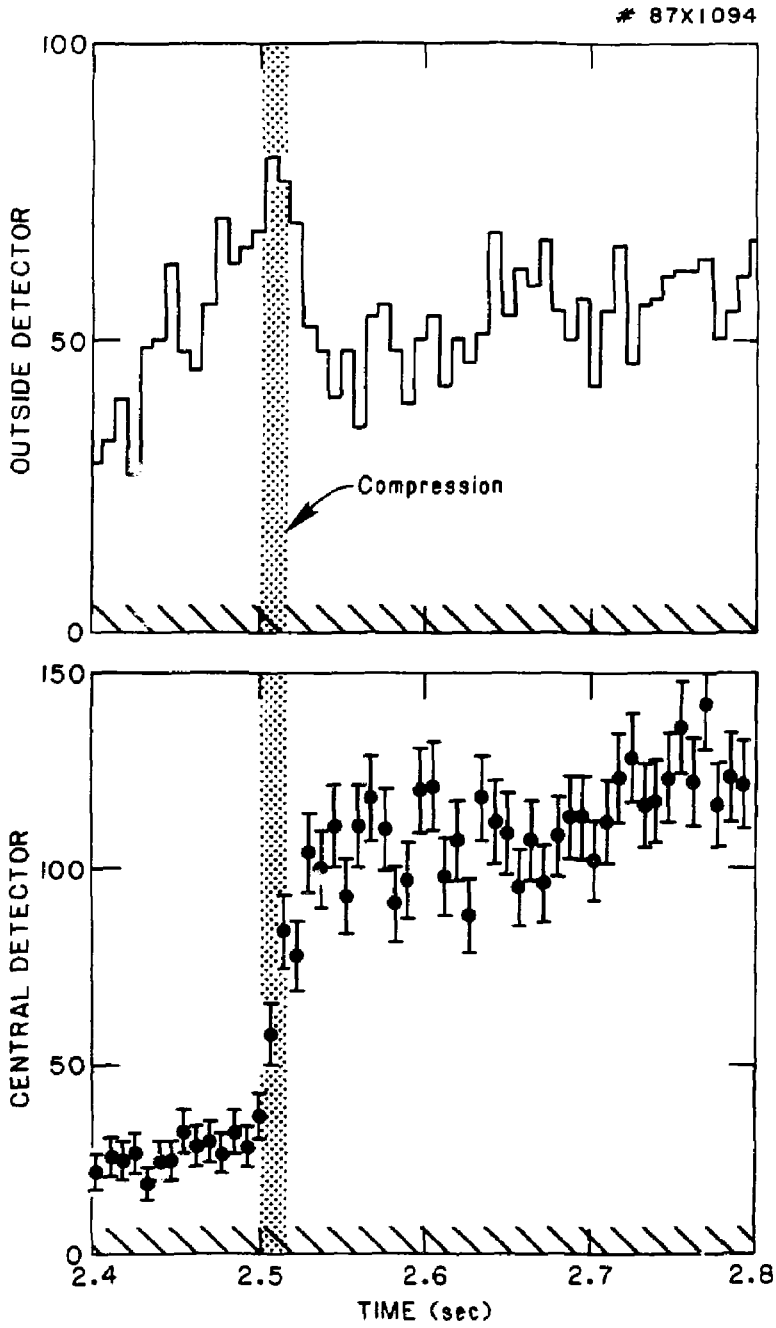
87X1094
100
50
0
OUTSIDE DETECTOR
Compression
150
100
50
0
CENTRAL DETECTOR
2.4
2.5
2.6
2.7
2.8
TIME (sec)

Fig. 10